Simulation and Hardware Implementation of Incremental Conductance MPPT With Direct Control Method Using Cuk Converter

Azadeh Safari and Saad Mekhilef, *Member, IEEE*

***Abstract*—This paper presents simulation and hardware implementation of incremental conductance (IncCond) maximum power point tracking (MPPT) used in solar array power systems with direct control method. The main difference of the proposed system to existing MPPT systems includes elimination of the proportional–integral control loop and investigation of the effect of simplifying the control circuit. Contributions are made in several aspects of the whole system, including converter design, system simulation, controller programming, and experimental setup. The resultant system is capable of tracking MPPs accurately and rapidly without steady-state oscillation, and also, its dynamic performance is satisfactory. The IncCond algorithm is used to track MPPs because it performs precise control under rapidly changing atmospheric conditions. MATLAB and Simulink were employed for simulation studies, and Code Composer Studio v3.1 was used to program a TMS320F2812 digital signal processor. The proposed system was developed and tested successfully on a photovoltaic solar panel in the laboratory. Experimental results indicate the feasibility and improved functionality of the system.**

***Index Terms*—Digital signal processor (DSP), incremental conductance (IncCond), maximum power point tracking (MPPT), photovoltaic (PV) system.**

I. Introduction

RECENTLY, energy generated from clean, efficient, and environmentally friendly sources has become one of the major challenges for engineers and scientists [1]. Among all renewable energy sources, solar power systems attract more attention because they provide excellent opportunity to generate electricity while greenhouse emissions are reduced [1]–[3]. It is also gratifying to lose reliance on conventional electricity generated by burning coal and natural gas. Regarding the endless aspect of solar energy, it is worth saying that solar energy is a unique prospective solution for energy crisis. However, despite all the aforementioned advantages of solar power systems, they do not present desirable efficiency [4], [5].

The efficiency of solar cells depends on many factors such as temperature, insolation, spectral characteristics of sunlight, dirt, shadow, and so on. Changes in insolation on panels due to fast climatic changes such as cloudy weather and increase in ambient temperature can reduce the photovoltaic (PV) array output power. In other words, each PV cell produces energy pertaining to its operational and environmental conditions [6], [7].

In addressing the poor efficiency of PV systems, some methods are proposed, among which is a new concept called "maximum power point tracking" (MPPT). All MPPT methods follow the same goal which is maximizing the PV array output power by tracking the maximum power on every operating condition.

A. MPPT Methods

There is a large number of algorithms that are able to track MPPs. Some of them are simple, such as those based on voltage and current feedback, and some are more complicated, such as perturbation and observation (P&O) or the incremental conductance (IncCond) method. They also vary in complexity, sensor requirement, speed of convergence, cost, range of operation, popularity, ability to detect multiple local maxima, and their applications [8]–[10].

Having a curious look at the recommended methods, hill climbing and P&O [11]–[16] are the algorithms that were in the center of consideration because of their simplicity and ease of implementation. Hill climbing [14], [17] is perturbation in the duty ratio of the power converter, and the P&O method [15], [18] is perturbation in the operating voltage of the PV array. However, the P&O algorithm cannot compare the array terminal voltage with the actual MPP voltage, since the change in power is only considered to be a result of the array terminal voltage perturbation. As a result, they are not accurate enough because they perform steady-state oscillations, which consequently waste the energy [8]. By minimizing the perturbation step size, oscillation can be reduced, but a smaller perturbation size slows down the speed of tracking MPPs. Thus, there are some disadvantages with these methods, where they fail under rapidly changing atmospheric conditions [19].

On the other hand, some MPPTs are more rapid and accurate and, thus, more impressive, which need special design and familiarity with specific subjects such as fuzzy logic [20] or neural network [21] methods. MPPT fuzzy logic controllers have good performance under varying atmospheric conditions and exhibit better performance than the P&O control method [8]; however, the main disadvantage of this method is that its effectiveness is highly dependent on the technical knowledge of the engineer in computing the error and coming up with

Manuscript received July 29, 2009; revised December 24, 2009 and March 3, 2010; accepted March 24, 2010. Date of publication April 29, 2010; date of current version March 11, 2011.

The authors are with the Department of Electrical Engineering, University of Malaya, Kuala Lumpur 50603, Malaysia (e-mail: azadehsafari2008@gmail.com; saad@um.edu.my).

Color versions of one or more of the figures in this paper are available online at http://ieeexplore.ieee.org.

Digital Object Identifier 10.1109/TIE.2010.2048834

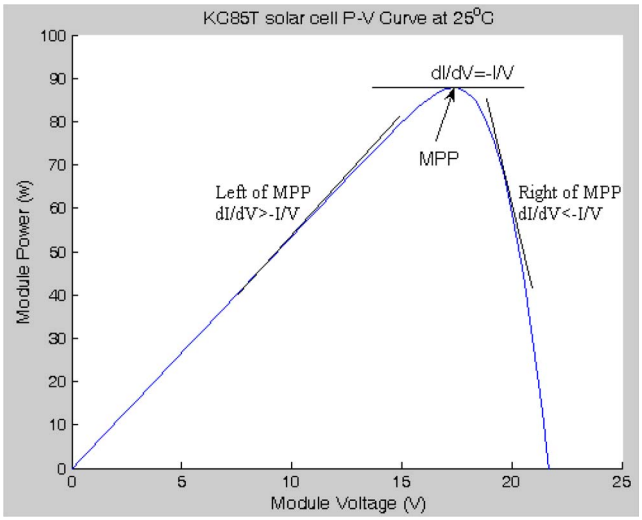

Fig. 1. Basic idea of the IncCond method on a P–V curve of a solar module.

the rule-based table. It is greatly dependent on how a designer arranges the system that requires skill and experience.

A similar disadvantage of the neural network method comes with its reliance on the characteristics of the PV array that change with time, implying that the neural network has to be periodically trained to guarantee accurate MPPs.

The IncCond method is the one which overrides over the aforementioned drawbacks. In this method, the array terminal voltage is always adjusted according to the MPP voltage. It is based on the incremental and instantaneous conductance of the PV module [6], [19], [22], [23].

Fig. 1 shows that the slope of the PV array power curve is zero at the MPP, increasing on the left of the MPP and decreasing on the right-hand side of the MPP. The basic equations of this method are as follows [24]:

$$\frac{dI}{dV} = -\frac{I}{V}, \qquad \text{at MPP} \tag{1}$$

$$\frac{dI}{dV} > -\frac{I}{V}, \qquad \text{left of MPP} \tag{2}$$

$$\frac{dI}{dV} < -\frac{I}{V}, \qquad \text{right of MPP} \tag{3}$$

where I and V are the PV array output current and voltage, respectively. The left-hand side of the equations represents the IncCond of the PV module, and the right-hand side represents the instantaneous conductance. From (1)–(3), it is obvious that when the ratio of change in the output conductance is equal to the negative output conductance, the solar array will operate at the MPP. In other words, by comparing the conductance at each sampling time, the MPPT will track the maximum power of the PV module. The accuracy of this method is proven in [8], where it mentions that the IncCond method can track the true MPPs independent of PV array characteristics. Also, Roman *et al.* [25] described it as the best MPPT method, where it has made a comprehensive comparison between P&O and the IncCond method with boost converter and shows that the efficiency of experimental results is up to 95%. In [10], efficiency was observed to be as much as 98.2%, but it is doubtful of the IncCond method reliability issues due to the noise of components.

TABLE I
COMPARISON OF COMMON MPPT METHODS

MPPT technique	Speed	Complexity	Reliability	Implementation
Fractional I_{sc}	Medium	Medium	Low	Digital/Analog
Fractional V_{oc}	Medium	Low	Low	Digital/Analog
IncCond	Varies	Medium	Medium	Digital
Hill climbing	Varies	Low	Medium	Digital/Analog
Fuzzy logic	Fast	High	Medium	Digital
Neural network	Fast	High	Medium	Digital

Some modifications and reformations were proposed on this method so far, but since this method inherently has a good efficiency, the aforementioned amendments increase the complexity and cost of the system and there was no remarkable change in system efficiency. In [6], the variable-step-size IncCond method has been compared with the fixed-step-size one. The variable step size with constant-voltage-tracking start-up system has a performance of 99.2%, while the fixed step size has good efficiency as much as 98.9% due to the chosen small step size. Hence, it was revealed that with proper step size selection, the efficiency of the IncCond method is satisfactory. Table I shows a detailed comparison of the major characteristics for the aforementioned MPPT methods, with a focus on speed of convergence, complexity of implementation, reliability to detect real MPPs with varying weather conditions, and preferred method for implementation.

B. Direct Control Method

Conventional MPPT systems have two independent control loops to control the MPPT. The first control loop contains the MPPT algorithm, and the second one is usually a proportional (P) or P–integral (PI) controller. The IncCond method makes use of instantaneous and IncCond to generate an error signal, which is zero at the MPP; however, it is not zero at most of the operating points. The main purpose of the second control loop is to make the error from MPPs near to zero [8]. Simplicity of operation, ease of design, inexpensive maintenance, and low cost made PI controllers very popular in most linear systems. However, the MPPT system of standalone PV is a nonlinear control problem due to the nonlinearity nature of PV and unpredictable environmental conditions, and hence, PI controllers do not generally work well [26].

In this paper, the IncCond method with direct control is selected. The PI control loop is eliminated, and the duty cycle is adjusted directly in the algorithm. The control loop is simplified, and the computational time for tuning controller gains is eliminated. To compensate the lack of PI controller in the proposed system, a small marginal error of 0.002 was allowed. The objective of this paper is to eliminate the second control loop and to show that sophisticated MPPT methods do

not necessarily obtain the best results, but employing them in a simple manner for complicated electronic subjects is considered necessary. The feasibility of the proposed system is investigated with a dc–dc converter configured as the MPPT. In [27], it was mentioned that the power extracted from PV modules with analog circuitry can only operate at the MPP in a predefined illumination level. Therefore, control action is done using a TMS320F2812 digital signal processor (DSP), which is specially designed for control actions. It generates pulsewidth modulation (PWM) waveform to control the duty cycle of the converter switch according to the IncCond algorithm.

II. PV Module and MPPT

The basic structural unit of a solar module is the PV cells. A solar cell converts energy in the photons of sunlight into electricity by means of the photoelectric phenomenon found in certain types of semiconductor materials such as silicon and selenium.

A single solar cell can only produce a small amount of power. To increase the output power of a system, solar cells are generally connected in series or parallel to form PV modules. PV module characteristics are comprehensively discussed in [3], [6], [11], [28], and [29], which indicate an exponential and nonlinear relation between the output current and voltage of a PV module. The main equation for the output current of a module is [6]

$$I_o = n_p I_{ph} - n_p I_{rs}\left[\exp\left(k_0 \frac{v}{n_s}\right) - 1\right] \tag{4}$$

where I_o is the PV array output current, V is the PV output voltage, $I_{\rm ph}$ is the cell photocurrent that is proportional to solar irradiation, $I_{\rm rs}$ is the cell reverse saturation current that mainly depends on temperature, K_o is a constant, n_s represents the number of PV cells connected in series, and n_p represents the number of such strings connected in parallel.

In (4), the cell photocurrent is calculated from

$$I_{\rm ph} = [I_{\rm scr} + k_i(T - T_r)]\,\frac{S}{100} \tag{5}$$

where

$I_{\rm scr}$ cell short-circuit current at reference temperature and radiation;
k_I short-circuit current temperature coefficient;
T_r cell reference temperature;
S solar irradiation in milliwatts per square centimeter.

Moreover, the cell reverse saturation current is computed from

$$I_{\rm rs} = I_{\rm rr}\left[\frac{T}{T_r}\right]^3 \exp\left(\frac{qE_G}{kA}\left[\frac{1}{T_r} - \frac{1}{T}\right]\right) \tag{6}$$

where

T_r cell reference temperature;
$I_{\rm rr}$ reverse saturation at T_r;
E_G band-gap energy of the semiconductor used in the cell.

For simulations and the experimental setup also, the KC85T module was chosen. The electrical parameters are tabulated in Table II, and the resultant curves are shown in Fig. 2(a) and (b). It shows the effect of varying weather conditions on MPP location at I–V and P–V curves. Fig. 3 shows the current-versus-voltage curve of a PV module. It gives an idea about the significant points on each I–V curve: open-circuit voltage, short-circuit current, and the operating point where the module performs the maximum power (MPP). This point is related to a voltage and a current that are Vmpp and Impp, respectively, and is highly dependent on solar irradiation and ambient temperature [7].

TABLE II
ELECTRICAL PARAMETERS OF KC85T MODULE

Maximum power (Pmax)	87w
Voltage at MPP (Vmpp)	17.4v
Current at MPP (Impp)	5.02A
Open circuit voltage (Voc)	21.7v
Short circuit current (Isc)	5.34A

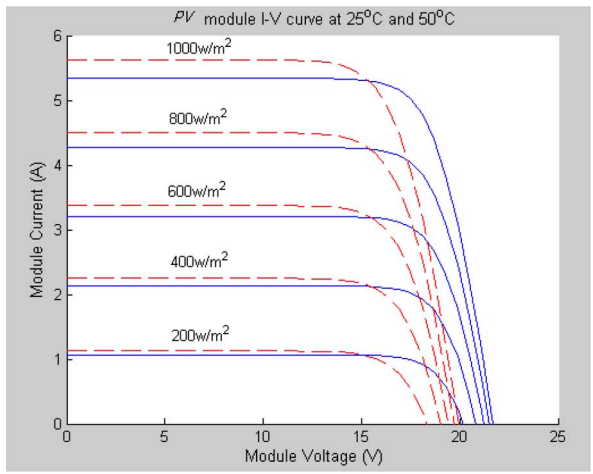

(a)

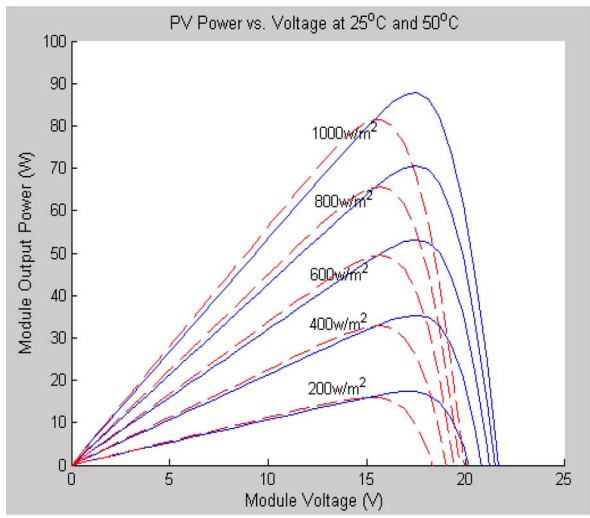

(b)

Fig. 2. Maximum power with varying weather conditions [−25 °C, −50 °C]. (a) I–V curves. (b) P–V curves.

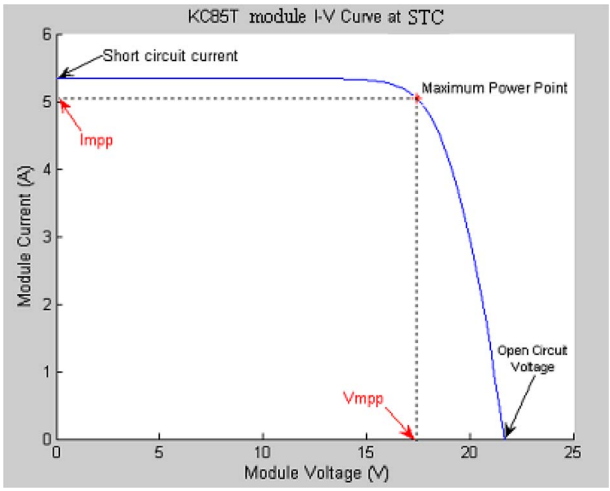

Fig. 3. Current-versus-voltage curve of a PV module.

In Fig. 2, it is clear that the MPP is located at the knee of the I–V curve, where the resistance is equal to the negative of differential resistance [25], [30]

$$\frac{V}{I} = -\frac{V}{I}. \tag{7}$$

This is following the general rule used in the P&O method, in which the slope of the PV curve at the MPP is equal to zero

$$\frac{dP}{dV} = 0. \tag{8}$$

Equation (8) can be rewritten as follows:

$$\frac{dP}{dV} = I \cdot \frac{dV}{dV} + V \cdot \frac{dI}{dV} \tag{9}$$

$$\frac{dP}{dV} = I + V \cdot \frac{dI}{dV} \tag{10}$$

and hence

$$I + V \cdot \frac{dI}{dV} = 0 \tag{11}$$

which is the basic idea of the IncCond algorithm.

One noteworthy point to mention is that (7) or (8) rarely occurs in practical implementation, and a small error is usually permitted [24]. The size of this permissible error (e) determines the sensitivity of the system. This error is selected with respect to the swap between steady-state oscillations and risk of fluctuating at a similar operating point.

It is suggested to choose a small and positive digit [24], [31]. Thus, (10) can be rewritten as

$$I + V \cdot \frac{dI}{dV} = e. \tag{12}$$

In this paper, the value of "e" was chosen as 0.002 on the basis of the trial-and-error procedure. The flowchart of the IncCond algorithm within the direct control method is shown in Fig. 4. According to the MPPT algorithm, the duty cycle (D) is calculated. This is the desired duty cycle that the PV module must operate on the next step. Setting a new duty cycle in the system is repeated according to the sampling time.

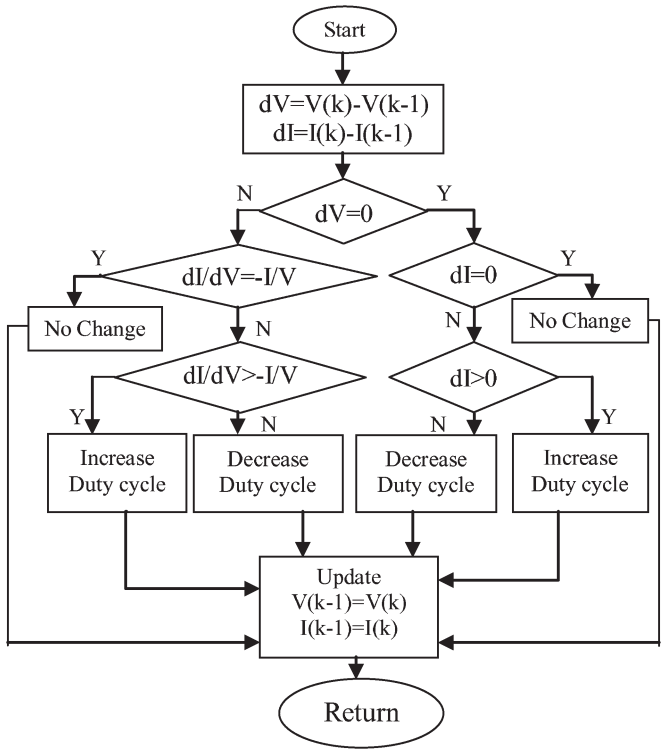

Fig. 4. Flowchart of the IncCond method with direct control.

III. Selecting Proper Converter

When proposing an MPP tracker, the major job is to choose and design a highly efficient converter, which is supposed to operate as the main part of the MPPT. The efficiency of switch-mode dc–dc converters is widely discussed in [1]. Most switching-mode power supplies are well designed to function with high efficiency.

Among all the topologies available, both Cuk and buck–boost converters provide the opportunity to have either higher or lower output voltage compared with the input voltage. Although the buck–boost configuration is cheaper than the Cuk one, some disadvantages, such as discontinuous input current, high peak currents in power components, and poor transient response, make it less efficient. On the other hand, the Cuk converter has low switching losses and the highest efficiency among nonisolated dc–dc converters. It can also provide a better output-current characteristic due to the inductor on the output stage. Thus, the Cuk configuration is a proper converter to be employed in designing the MPPT.

Figs. 5 and 6 show a Cuk converter and its operating modes, which is used as the power stage interface between the PV module and the load. The Cuk converter has two modes of operation. The first mode of operation is when the switch is closed (ON), and it is conducting as a short circuit. In this mode, the capacitor releases energy to the output. The equations for the switch conduction mode are as follows:

$$v_{L1} = V_g \tag{13}$$

$$v_{L2} = -v_1 - v_2 \tag{14}$$

$$i_{c1} = i_2 \tag{15}$$

$$i_{c2} = i_2 - \frac{v_2}{R}. \tag{16}$$

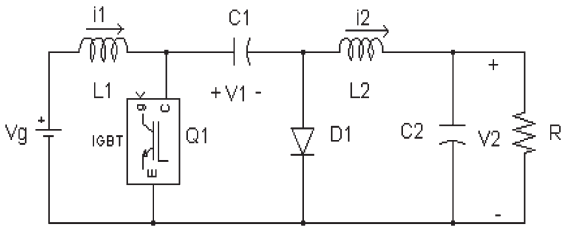

Fig. 5. Electrical circuit of the Cuk converter used as the PV power-stage interface.

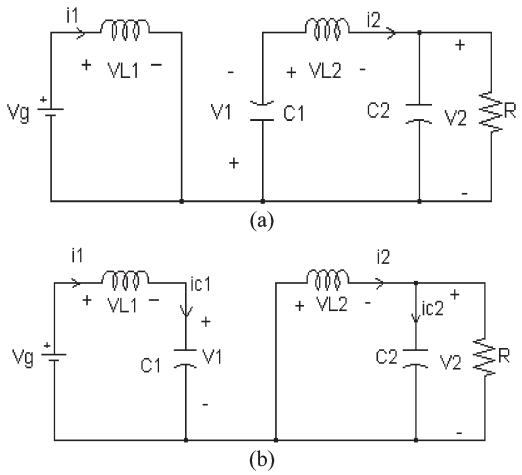

Fig. 6. Cuk converter with (a) switch ON and (b) switch OFF.

On the second operating mode when the switch is open (OFF), the diode is forward-biased and conducting energy to the output. Capacitor C1 is charging from the input. The equations for this mode of operation are as follows:

$$v_{L1} = V_g - v_1 \tag{17}$$

$$v_{L2} = -v_2 \tag{18}$$

$$i_{c1} = i_1 \tag{19}$$

$$i_{c2} = i_2 - \frac{v_2}{R}. \tag{20}$$

The principles of Cuk converter operating conditions state that the average values of the periodic inductor voltage and capacitor current waveforms are zero when the converter operates in steady state.

The relations between output and input currents and voltages are given in the following:

$$\frac{V_o}{V_{\text{in}}} = -\left(\frac{D}{1-D}\right) \tag{21}$$

$$\frac{I_{\text{in}}}{I_o} = -\left(\frac{D}{1-D}\right). \tag{22}$$

Some analyses of Cuk converter specifications are provided in [32], and a comparative study on different schemes of switching converters is presented in the literature [33].

The components for the Cuk converter used in simulation and the hardware setup were selected as follows:

1) input inductor L1 $= 5$ mH;
2) capacitor C1 (PV side) $= 47$ μf;
3) filter inductor L2 $= 5$ mH;
4) switch: insulated-gate bipolar transistor [(IGBT)—IRG4PH50U];
5) freewheeling diode: RHRG30120;
6) capacitor C2 (filter side) $= 1$ μF;
7) resistive load $= 10$ Ω;
8) switching frequency $= 10$ kHz;
9) controller: TMS320F2812 DSP.

The components for the measurement circuit are as follows:

1) voltage transducer: LV25-P;
2) current transducer: LA25-NP.

The power circuit of the proposed system consists of a Cuk converter and a gate drive, and the control of the switching is done using the control circuit. The control tasks involve measuring the analog voltage and current of the PV module using current and voltage sensors, convert them to digital using an ADC, process the obtained information in a microcontroller, then them compare to the predefined values to determine the next step, revert the PWM to the gate drive, and hence control the switching of IGBTs. The control loop frequently happens with respect to the sampling time, and the main program continues to track the MPPs.

IV. Simulation Results

The diagram of the closed-loop system designed in MATLAB and Simulink is shown in Fig. 7, which includes the PV module electrical circuit, the Cuk converter, and the MPPT algorithm. The converter components are chosen according to the values presented in Section II. The PV module is modeled using electrical characteristics to provide the output current and voltage of the PV module. The provided current and voltage are fed to the converter and the controller simultaneously.

The PI control loop is eliminated, and the duty cycle is adjusted directly in the algorithm. To compensate the lack of PI controller in the proposed system, a small marginal error of 0.002 is allowed.

To test the system operation, the condition of changing irradiation was modeled. The temperature is constant at 25 °C, and the illumination level is varying between two levels. The first illumination level is 1000 W/m^2; at $t = 0.4$ s, the illumination level suddenly changes to 400 W/m^2 and then back to 1000 W/m^2 at $t = 0.8$ s.

An illustration of the relationship between the duty cycle and PV output power is shown in Fig. 8(a) and (b) to demonstrate the effectiveness of the algorithm mentioned in the flowchart. Fig. 8(a) shows the change in duty cycle adjusted by the MPPT to extract the maximum power from the module.

The results in Fig. 8(b) show that the output power at $G = 1000$ and 400 W/m^2 are 87 and 35 W, respectively, which are absolutely the desired output power from Fig. 3(b). It also shows that the system provides the best desirable tradeoff between the two irradiation levels.

V. Experimental Setup

To verify the functionality and performance of the proposed system shown in Fig. 7, a prototype of the Cuk converter and

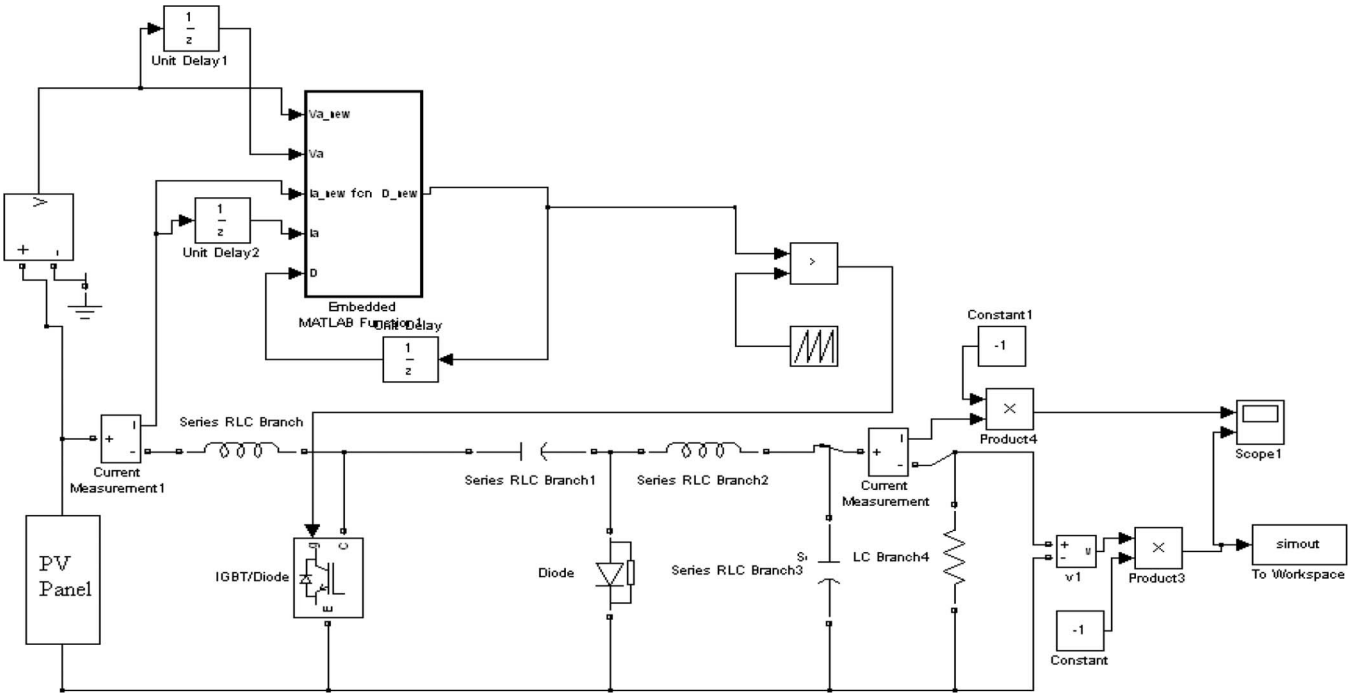

Fig. 7. Diagram of the closed-loop system.

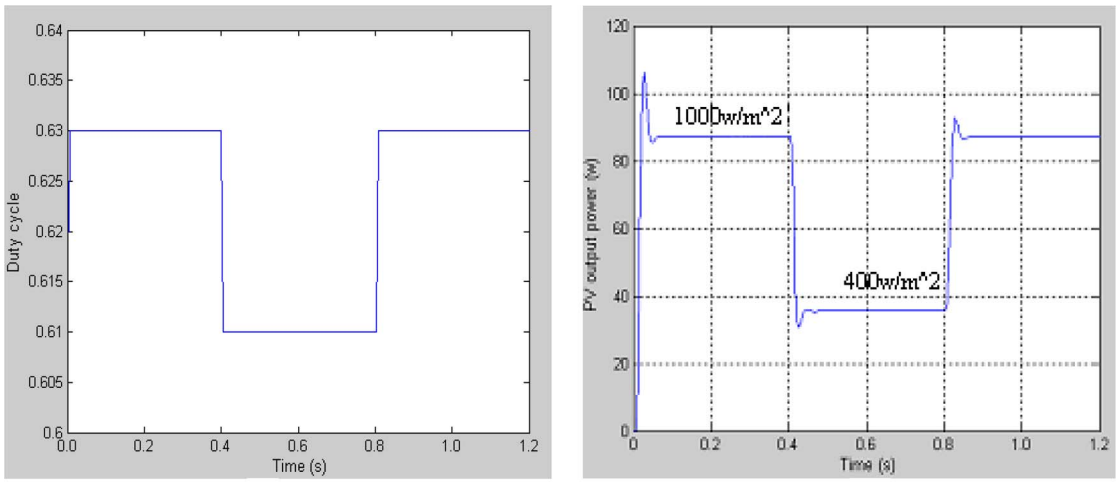

(a) (b)

Fig. 8. Change in (a) duty cycle and (b) power of the system due to the change in illumination level.

control circuit was implemented. The TMS320F2812 DSP was used to provide the control signals for the Cuk converter.

The C code of the IncCond algorithm and PWM scheme is built, debugged, and run with the help of the DSP development tool, Code Composer Studio software.

Voltage measurement is required at the point where the PV module output is connected to the input of the Cuk converter. The voltage at this point is the operating voltage of the PV module. On the other hand, current measurement is also necessary to indicate the generated current of the PV module on each operating point. It is particularly important to determine the atmospheric condition, which is vital in connection with the accuracy of MPP tracking. For the aforementioned reason, the PV array voltage and current are measured using Hall-effect sensors, which were pointed out in Section II. However, since the DSP board cannot tolerate more than 3.3 V, the measured values will be scaled down to be compatible with the DSP voltage rating.

The PV array is operating around an open-circuit voltage (80 V) before connecting the PV to the load through the MPPT circuit. When the PV is connected to the MPPT circuit, it does not operate at the mentioned voltage anymore, and the voltage drops to a new point instantly. This new operating voltage depends on the impedance of the load. In order to move the new operating point to the MPP, the control rules of IncCond within the direct control loop will assume the function.

Solar modules are usually connected together to attain high output power. There are two general types of connecting modules: series and parallel. The type of connection totally depends on the application where large current or voltage is required.

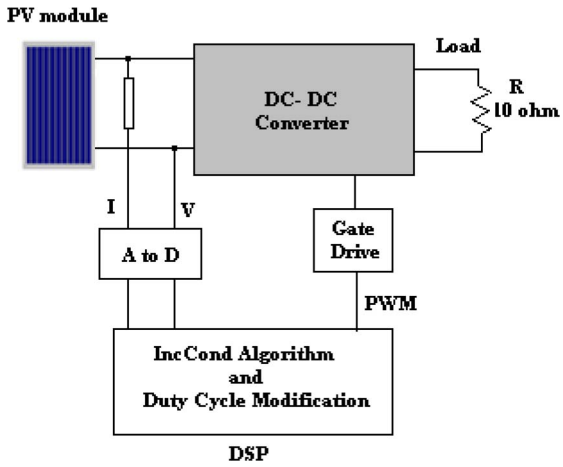

Fig. 9. Direct control method used in the MPPT.

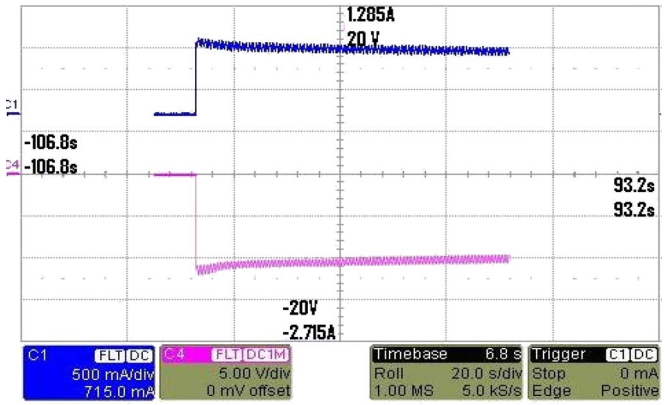

Fig. 10. Initial current and voltage after connecting to the MPPT with one module ($-I$ = upper waveform, V = lower waveform).

The purpose in the series configuration is to increase the output voltage, while the parallel connection is made to increase the current. The interconnection of cells in a module itself is mostly in series to provide higher voltage.

When modules are connected in series, the total voltage is the sum of each module voltage, but the current stays constant, and it is the smallest current of a module available in the configuration. In the hardware configuration, there are four modules connected in series. Fig. 9 shows the block diagram of the MPPT system with direct control using a Cuk converter.

The sampling time of the system is chosen to be 0.2 s, which is the required time for the designed Cuk converter to reach the steady-state condition. The step size of duty cycle is chosen to be 0.2, so the converter can smoothly track the MPP.

Fig. 10 shows the initial waveforms of current and voltage after connecting the PV module to the circuit. There is some overshoot in both waveforms, which was predicted from the simulation results in Fig. 8(b).

After conducting an in-depth investigation on system performance under rapidly varying illumination levels, the numbers of modules were changed from three to two. The variations of the voltage and power of the system are shown in Figs. 11 and 12, respectively.

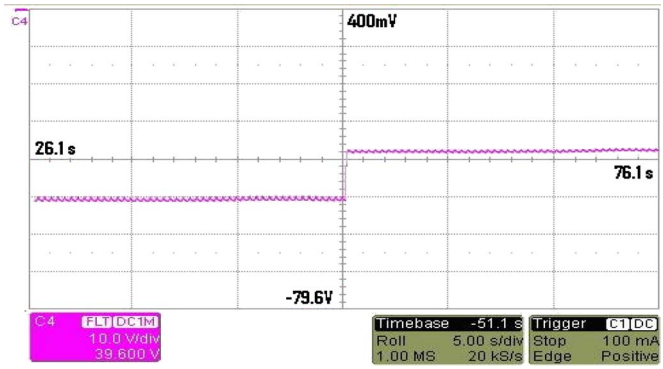

Fig. 11. Change in voltage when the number of PV modules is decreased from three to two.

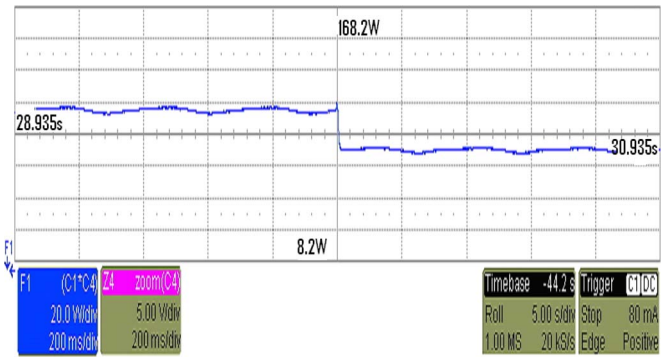

Fig. 12. Change in power when the number of PV modules is decreased from three to two.

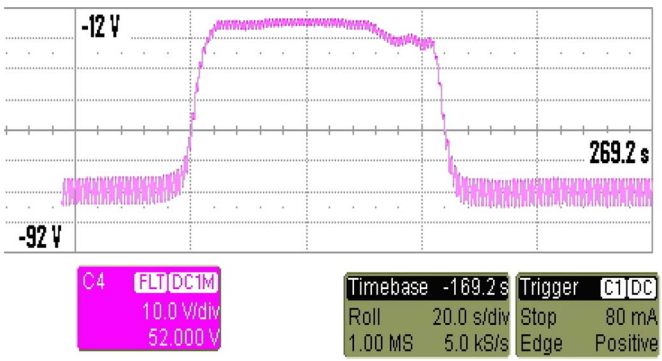

Fig. 13. PV array voltage response for varying the illumination level.

Fig. 13 shows the voltage of the PV for decreasing the irradiation level and thereafter increasing it. It shows the dynamic performance of the system.

VI. Conclusion

In this paper, a fixed-step-size IncCond MPPT with direct control method was employed, and the necessity of another control loop was eliminated. The proposed system was simulated and constructed, and the functionality of the suggested control concept was proven. From the results acquired during the simulations and hardware experiments, it was confirmed that, with a well-designed system including a proper converter and selecting an efficient and proven algorithm, the implementation of MPPT is simple and can be easily constructed to

achieve an acceptable efficiency level of the PV modules. The results also indicate that the proposed control system is capable of tracking the PV array maximum power and thus improves the efficiency of the PV system and reduces low power loss and system cost.

REFERENCES

[1] R.-J. Wai, W.-H. Wang, and C.-Y. Lin, "High-performance stand-alone photovoltaic generation system," *IEEE Trans. Ind. Electron.*, vol. 55, no. 1, pp. 240–250, Jan. 2008.

[2] W. Xiao, W. G. Dunford, P. R. Palmer, and A. Capel, "Regulation of photovoltaic voltage," *IEEE Trans. Ind. Electron.*, vol. 54, no. 3, pp. 1365–1374, Jun. 2007.

[3] N. Mutoh and T. Inoue, "A control method to charge series-connected ultra electric double-layer capacitors suitable for photovoltaic generation systems combining MPPT control method," *IEEE Trans. Ind. Electron.*, vol. 54, no. 1, pp. 374–383, Feb. 2007.

[4] R. Faranda, S. Leva, and V. Maugeri, *MPPT Techniques for PV Systems: Energetic and Cost Comparison*. Milano, Italy: Elect. Eng. Dept. Politecnico di Milano, 2008, pp. 1–6.

[5] Z. Yan, L. Fei, Y. Jinjun, and D. Shanxu, "Study on realizing MPPT by improved incremental conductance method with variable step-size," in *Proc. IEEE ICIEA*, Jun. 2008, pp. 547–550.

[6] F. Liu, S. Duan, F. Liu, B. Liu, and Y. Kang, "A variable step size INC MPPT method for PV systems," *IEEE Trans. Ind. Electron.*, vol. 55, no. 7, pp. 2622–2628, Jul. 2008.

[7] F. M. González-Longatt, "Model of photovoltaic module in Matlab," in *2do congreso iberoamericano de estudiantes de ingenierıacute;a eléctrica, electrónica y computación, ii cibelec*, 2005, pp. 1–5.

[8] T. Esram and P. L. Chapman, "Comparison of photovoltaic array maximum power point tracking techniques," *IEEE Trans. Energy Convers.*, vol. 22, no. 2, pp. 439–449, Jun. 2007.

[9] V. Salas, E. Olias, A. Barrado, and A. Lazaro, "Review of the maximum power point tracking algorithms for stand-alone photovoltaic systems," *Sol. Energy Mater. Sol. Cells*, vol. 90, no. 11, pp. 1555–1578, Jul. 2006.

[10] G. Petrone, G. Spagnuolo, R. Teodorescu, M. Veerachary, and M. Vitelli, "Reliability issues in photovoltaic power processing systems," *IEEE Trans. Ind. Electron.*, vol. 55, no. 7, pp. 2569–2580, Jul. 2008.

[11] C. Hua, J. Lin, and C. Shen, "Implementation of a DSP-controlled photovoltaic system with peak power tracking," *IEEE Trans. Ind. Electron.*, vol. 45, no. 1, pp. 99–107, Feb. 1998.

[12] T. Noguchi, S. Togashi, and R. Nakamoto, "Short-current pulse-based maximum-power-point tracking method for multiple photovoltaic-and-converter module system," *IEEE Trans. Ind. Electron.*, vol. 49, no. 1, pp. 217–223, Feb. 2002.

[13] N. Mutoh, M. Ohno, and T. Inoue, "A method for MPPT control while searching for parameters corresponding to weather conditions for PV generation systems," *IEEE Trans. Ind. Electron.*, vol. 53, no. 4, pp. 1055–1065, Jun. 2006.

[14] N. Femia, G. Petrone, G. Spagnuolo, and M. Vitelli, "Optimization of perturb and observe maximum power point tracking method," *IEEE Trans. Power Electron.*, vol. 20, no. 4, pp. 963–973, Jul. 2005.

[15] N. Femia, D. Granozio, G. Petrone, G. Spagnuolo, and M. Vitelli, "Predictive & adaptive MPPT perturb and observe method," *IEEE Trans. Aerosp. Electron. Syst.*, vol. 43, no. 3, pp. 934–950, Jul. 2007.

[16] E. Koutroulis, K. Kalaitzakis, and N. C. Voulgaris, "Development of a microcontroller-based, photovoltaic maximum power point tracking control system," *IEEE Trans. Power Electron.*, vol. 16, no. 1, pp. 46–54, Jan. 2001.

[17] S. Jain and V. Agarwal, "A new algorithm for rapid tracking of approximate maximum power point in photovoltaic systems," *IEEE Power Electron. Lett.*, vol. 2, no. 1, pp. 16–19, Mar. 2004.

[18] A. Pandey, N. Dasgupta, and A. K. Mukerjee, "Design issues in implementing MPPT for improved tracking and dynamic performance," in *Proc. 32nd IECON*, Nov. 2006, pp. 4387–4391.

[19] K. H. Hussein, I. Muta, T. Hoshino, and M. Osakada, "Maximum photovoltaic power tracking: An algorithm for rapidly changing atmospheric conditions," *Proc. Inst. Elect. Eng.—Gener., Transmiss. Distrib.*, vol. 142, no. 1, pp. 59–64, Jan. 1995.

[20] T.-F. Wu, C.-H. Chang, and Y.-H. Chen, "A fuzzy-logic-controlled single-stage converter for PV-powered lighting system applications," *IEEE Trans. Ind. Electron.*, vol. 47, no. 2, pp. 287–296, Apr. 2000.

[21] M. Veerachary, T. Senjyu, and K. Uezato, "Neural-network-based maximum-power-point tracking of coupled-inductor interleaved-boost-converter-supplied PV system using fuzzy controller," *IEEE Trans. Ind. Electron.*, vol. 50, no. 4, pp. 749–758, Aug. 2003.

[22] B. Liu, S. Duan, F. Liu, and P. Xu, "Analysis and improvement of maximum power point tracking algorithm based on incremental conductance method for photovoltaic array," in *Proc. IEEE PEDS*, 2007, pp. 637–641.

[23] Y.-C. Kuo, T.-J. Liang, and J.-F. Chen, "Novel maximum-power-point-tracking controller for photovoltaic energy conversion system," *IEEE Trans. Ind. Electron.*, vol. 48, no. 3, pp. 594–601, Jun. 2001.

[24] D. Sera, T. Kerekes, R. Teodorescu, and F. Blaabjerg, *Improved MPPT Algorithms for Rapidly Changing Environmental Conditions*. Aalborg, Denmark: Aalborg Univ./Inst. Energy Technol., 2006.

[25] E. Roman, R. Alonso, P. Ibanez, S. Elorduizapatarietxe, and D. Goitia, "Intelligent PV module for grid-connected PV systems," *IEEE Trans. Ind. Electron.*, vol. 53, no. 4, pp. 1066–1073, Jun. 2006.

[26] F. Salem, M. S. Adel Moteleb, and H. T. Dorrah, "An enhanced fuzzy-PI controller applied to the MPPT problem," *J. Sci. Eng.*, vol. 8, no. 2, pp. 147–153, 2005.

[27] M. Fortunato, A. Giustiniani, G. Petrone, G. Spagnuolo, and M. Vitelli, "Maximum power point tracking in a one-cycle-controlled single-stage photovoltaic inverter," *IEEE Trans. Ind. Electron.*, vol. 55, no. 7, pp. 2684–2693, Jul. 2008.

[28] I.-S. Kim, M.-B. Kim, and M.-J. Youn, "New maximum power point tracker using sliding-mode observer for estimation of solar array current in the grid-connected photovoltaic system," *IEEE Trans. Ind. Electron.*, vol. 53, no. 4, pp. 1027–1035, Jun. 2006.

[29] W. Xiao, M. G. J. Lind, W. G. Dunford, and A. Capel, "Real-time identification of optimal operating points in photovoltaic power systems," *IEEE Trans. Ind. Electron.*, vol. 53, no. 4, pp. 1017–1026, Jun. 2006.

[30] J.-H. Park, J.-Y. Ahn, B.-H. Cho, and G.-J. Yu, "Dual-module-based maximum power point tracking control of photovoltaic systems," *IEEE Trans. Ind. Electron.*, vol. 53, no. 4, pp. 1036–1047, Jun. 2006.

[31] W. Wu, N. Pongratananukul, W. Qiu, K. Rustom, T. Kasparis, and I. Batarseh, "DSP-based multiple peak power tracking for expandable power system," in *Proc. 18th Annu. IEEE Appl. Power Electron. Conf. Expo.*, Feb. 2003, vol. 1, pp. 525–530.

[32] D. Maksimovic and S. Cuk, "A unified analysis of PWM converters in discontinuous modes," *IEEE Trans. Power Electron.*, vol. 6, no. 3, pp. 476–490, Jul. 1991.

[33] K. K. Tse, B. M. T. Ho, H. S.-H. Chung, and S. Y. R. Hui, "A comparative study of maximum-power-point trackers for photovoltaic panels using switching-frequency modulation scheme," *IEEE Trans. Ind. Electron.*, vol. 51, no. 2, pp. 410–418, Apr. 2004.

Azadeh Safari received the B.Eng. degree in electrical engineering from Karaj Azad University, Karaj, Iran, in 2006, and the M.E. degree in electromanufacturing engineering, by course work and dissertation, from the University of Malaya, Kuala Lumpur, Malaysia, in 2009.

She is currently with the Department of Electrical Engineering, University of Malaya. Her research interests include the development of electronic circuits for renewable energy systems, solar power electronics, and power converters.

Ms. Safari is a member of the Organization for Engineering Order of Building, Tehran, Iran.

Saad Mekhilef (M'01) received the B.Eng. degree in electrical engineering from the University of Setif, Setif, Algeria, in 1995 and the Master of Engineering Science and Ph.D. degrees from the University of Malaya, Kuala Lumpur, Malaysia, in 1998 and 2003, respectively.

He is currently an Associate Professor with the Department of Electrical Engineering, University of Malaya. He is the author and coauthor of more than 100 publications in international journals and proceedings. He is actively involved in industrial consultancy for major corporations in power electronic projects. His research interests include power conversion techniques, control of power converters, renewable energy, and energy efficiency.